
APPLIED ELECTROCHEMISTRY
AND METAL CORROSION PROTECTION

Structuring in the Formation Technology of Electrode Material Based on Nafion Proton-Conducting Polymer and Thermally Expanded Graphite Containing Platinum Nanoparticles on Carbon Black

A. O. Krasnova, N. V. Glebova, D. V. Zhilina, and A. A. Nechitailov*

Ioffe Physical Technical Institute, Russian Academy of Sciences, ul. Politekhnikeskaya 26, St. Petersburg, 194021 Russia
**e-mail: aan.shuv@mail.ioffe.ru*

Received March 9, 2016

Abstract—Laboratory production technique is described for fabrication of an electrode material containing platinum nanoparticles on carbon black, proton-conducting polymer Nafion, and thermally expanded graphite for direct-energy-conversion systems (fuel cells, electrolyzers, electrochemical sensors). Results of a study of the material by differential thermal analysis are presented. Scanning and transmission electron microscopy was used to examine the structure of the material, and its elemental composition was determined by the EDX method. Dependences of the porosity of the material on its composition are presented.

DOI: 10.1134/S1070427217030065

One of development avenues for production techniques of electrochemical systems for hydrogen power engineering consists in studying and implementing new nanostructured materials as functional additives for modification of the target characteristics. Graphene and graphene-like materials are of interest owing to their structural features (low dimension, large specific surface area), high electrical conductivity, and high porosity (thermally expanded graphite). Therefore, modern studies in the field of electrode materials for electrochemical devices with the use of graphene-like materials are represented by a considerable number of publications. For example, it has been reported [1] that the electrode material based on platinum nanoparticles deposited on the surface of graphene can be successfully used as a material for electrodes of an oxygen-hydrogen fuel cell. The review [2] summarized techniques for production of catalysts for fuel cells, developed during the last 15 years. The attention was focused on solid-polymer fuel cells. It is noted that, being a material with high chemical stability and making it possible to form prescribed structures of metallic nanoparticles

on its surface, graphene is promising as a support for platinum. It was noted in [3] that graphene is promising as a support for the platinum catalyst because of its corrosion resistance and strongly developed surface. This circumstance enables fabrication of electrocatalysts with high platinum utilization efficiency and long service life. The review [4], which has 103 references and covers the period of time from 2007 to 2015, described the tendencies in studying the application of various graphene materials in electrodes, electrolytes, and bipolar plates of solid-polymer fuel cells. It was noted that the use of graphene in solid-polymer fuel cells made it possible to substantially raise the electronic and ionic conductivity, improve the corrosion resistance, and enlarge the electrochemically active surface area, depending on the fuel-cell component in which graphene is used. At the same time, it was mentioned that the main difficulty in application of graphene is the need to use additional components for separating its sheets. It was noted in the report [5] describing modern methods for fabrication of nanocomposites for fuel cells on the basis of graphene-like materials that, owing to the unique properties of graphene,

such as its 2D structure, large specific surface area, and high electrical conductivity, it is considered promising for application in electrodes of electrochemical devices (fuel cell, lithium batteries, supercapacitors). Methods have been described for obtaining nanocomposites based on graphene and nanostructured metals, which include molecular-beam epitaxy, chemical reduction, sol-gel technique, electrochemical deposition, etc. The review [6] systematized the available evidence on how the magnetic sputtering method can be used to synthesize electrocatalysts and form protective coatings, analyzed the influence exerted by the process parameters on the properties of thus deposited coatings, and gave optimization recommendations. Particular attention was given to new nanocarbon supports (graphene, nanotubes).

The review [7] analyzed 144 reports containing present-day data on the application of graphene materials in composite membranes, including those for fuel cells. It was noted that graphene has a large potential for application in composite membranes on its basis.

In [8], thermally expanded graphite (TEG) was used as component of current-collector plates of a fuel cell for raising their electrical conductivity. In [9, 10], the functional opportunities for application of TEG in electrodes of chemical power cells were analyzed. It was experimentally demonstrated that using TEG as binder in an inert cathode of a backup element and in a manganese dioxide electrode for a lithium power cell improves their discharge characteristics.

Thus, our analysis of the modern scientific literature suggests that graphene-like materials are promising for application in the fuel-cell technology. At the same time, the main trend as regards the electrodes consists in using graphene-like materials as a support for nanostructured metals. The positive effect is provided in this case by the high corrosion resistance, large specific surface area, and high electrical conductivity of graphene. At the same time, studies of the structuring effect in application of graphene-like materials as functional additives in the production technique of composite electrodes have been little reported in the scientific literature. We suggested a new scientific approach, which consists in that TEG is used just as a structuring additive to the electrode material. It has been reported previously [11] that carbon nanofibers were used as a highly porous material as a structuring additive to the cathode of a hydrogen fuel cell. This made it possible to reduce the gas-diffusion resistance of the electrode and make larger the surface

area of platinum that was accessible to reagents. TEG is of interest for further development of the area associated with using nanostructured carbon materials as electrode structure modifiers because it has, in addition to the comparatively high chemical stability and high electrical conductivity, a high porosity and developed surface. At the same time, TEG is a material of the same chemical nature as carbon black. Owing to this circumstance, it is no need to remove the structuring material, in contrast to the technology of the well-known skeletal catalysts or in modification of the electrode surface [12].

To create materials with controlled characteristics, which are of practical importance for development of effective electrodes and reduction of the specific expenditure of platinum, it is necessary to study the relationship between the technology, structure, and characteristics of these materials.

The goal of our study was to examine the fundamental aspects of the relationship between the technology, composition, and structure of a composite electrode containing the proton-conducting polymer Nafion and nanostructured platinum on carbon black in modification of the porous structure via introduction of TEG.

EXPERIMENTAL

As starting materials were used the following components: carbon black of Vulcan XC-72 type with specific surface area of $250 \text{ m}^2 \text{ g}^{-1}$, platinized carbon black of Vulcan XC-72 type, and commercial product of the E-TEK type [13]. The content of platinum was 40%, and the characteristic particle size and the specific surface area of platinum were 2.8 nm and $100 \text{ m}^2 \text{ g}^{-1}$, respectively. The ionomer was introduced into the electrode material by using the commercial product, Ion Power Inc. Dupont DE2020, which is a 20% water-propanol solution of Nafion. The carbon material [14] was used as TEG. Membrane-electrode assemblies were fabricated on an MF4-SK proton-conducting membrane manufactured by Plastpolimer OAO.

We used the following technological and measuring equipment: Milaform MM-5M magnetic rabble, Branson 3510 ultrasonic bath, thickness meter with scale unit of $1 \mu\text{m}$, Mettler Toledo XP205DR analytical balance, and Ika C-MAG HP 7 hot plate with thermal control unit.

The electrode materials were prepared by the two-step technique: in the first stage, we performed a preliminary mechanical mixing of the starting components (platinized

carbon black, TEG, and Nafion) in an isopropanol–water mixture in a magnetic rabble with a core insulated in a plastic case and rotation speed of ~400 rpm for ~0.5 h until a visually homogeneous (without visible lumps) paste was formed; in the second stage, the mixture was ultrasonically dispersed in the ultrasonic bath until a stable homogeneous dispersion of the components was formed.

The working Nafion solution containing 2% main substance in an isopropanol : water mixture taken in a 1 : 1 volume ratio was mixed with the equal amount of water and then poured onto the solid components.

The s : l solid-to-liquid phase ratio in the final dispersion (catalytic ink) was in the range from 1 : 40 to 1 : 80. The ultrasonic treatment in the ultrasonic bath with working ultrasound frequency of 40 kHz at a power of 130 W was performed during 30–50 h until a visually homogeneous dispersion was obtained.

A part of the dispersion was dried in air to control the composition by thermogravimetric analysis.

To examine the porosity of the resulting materials, we fabricated membrane-electrode assemblies from the catalytic ink. We used for this purpose the method of pasting of the electrode material onto a proton-conducting membrane through a steel mask with 1 × 1 cm window, with the membrane thermostated at a temperature of 85°C [15, 16]. The amount of the thus deposited material was determined by gravimetry.

The porosity of the electrodes fabricated on the surface of the proton-conducting membrane was calculated by the relations

$$P = \frac{V_1 - V_s}{V_1}, \quad (1)$$

$$V_s = \sum_{i=1}^n \frac{nV_1\omega_i}{d_i}, \quad (2)$$

where P is the porosity; V_1 and V_s , volumes of the layer (electrode) and of the sum of the solid components in this layer, respectively; m_i , layer mass; ω_i , mass fraction of i th component in the layer; and d_i , density of i th component.

To calculate the volume of the layer, we measured its thickness with a thickness meter at ten places and averaged these values, the layer area was 1 cm², and the thickness was in the range 4–65 μm.

We made several assumptions in the calculations. Because Nafion is a gas-insulating material and we

examined in the study the porous structure involved in the gas transport, its porosity was taken to be zero. The density of dry Nafion was taken to be 2.0 g cm⁻³ on the basis of the results of our measurements of the dry membrane and published data [17, 18]. The densities of the carbon materials Vulcan XC-72 and TEG were taken to be 2.2 g cm⁻³, and that of platinum, 21.45 g cm⁻³.

The thermogravimetric measurements were made on a Mettler Toledo TGA/DSC 1 derivatograph with Star System software (Switzerland). Air was blown through the chamber of the derivatograph at a flow rate of 30 cm³ min⁻¹, and the temperature was raised at a constant rate of 10 deg min⁻¹ within the temperature range 35–1000°C.

The electrochemical behavior of the material was studied by the method of cyclic voltammetry (CVA) on a stationary disk electrode. A dispersion of a sample in an isopropanol-water medium was applied to the polished surface (0.07 cm²) of a glassy-carbon disk electrode and dried in air. Measurements were made in 0.5 M sulfuric acid, with the solution being in equilibrium with air. The electrode potential of the sample was multiply cycled within the range from –150 to +1000 mV relative to a silver chloride reference electrode at a rate of 50 mV s⁻¹. The electrode potential of the sample was measured relative to the silver chloride reference electrode.

The analytical measurements were optimized for a microscopic study within the approach reported in [19]. Prior to measurements, powder samples were placed on copper grids 3 mm in diameter, fixed in a special holder. The structure of the samples was examined under natural conditions in order to eliminate surface effects caused by deposition of a conducting layer [20]. The microstructure of the samples was examined by field-emission scanning transmission electron microscopy (FE-STEM) on a Hitachi SU8000 electron microscope. Images were obtained in the transmitted-electron (light-field) mode at accelerating voltage of 30 kV.

RESULTS AND DISCUSSION

Thermal stability of TEG. Figure 1 shows derivatograms characterizing the thermal stability and specific features of the thermal oxidation of TEG in comparison with Vulcan XC-72 carbon black.

It can be seen in Fig. 1 that the oxidation of TEG is accompanied by three steps in the thermogravimetric (TG) curve and by the corresponding peaks in the differential

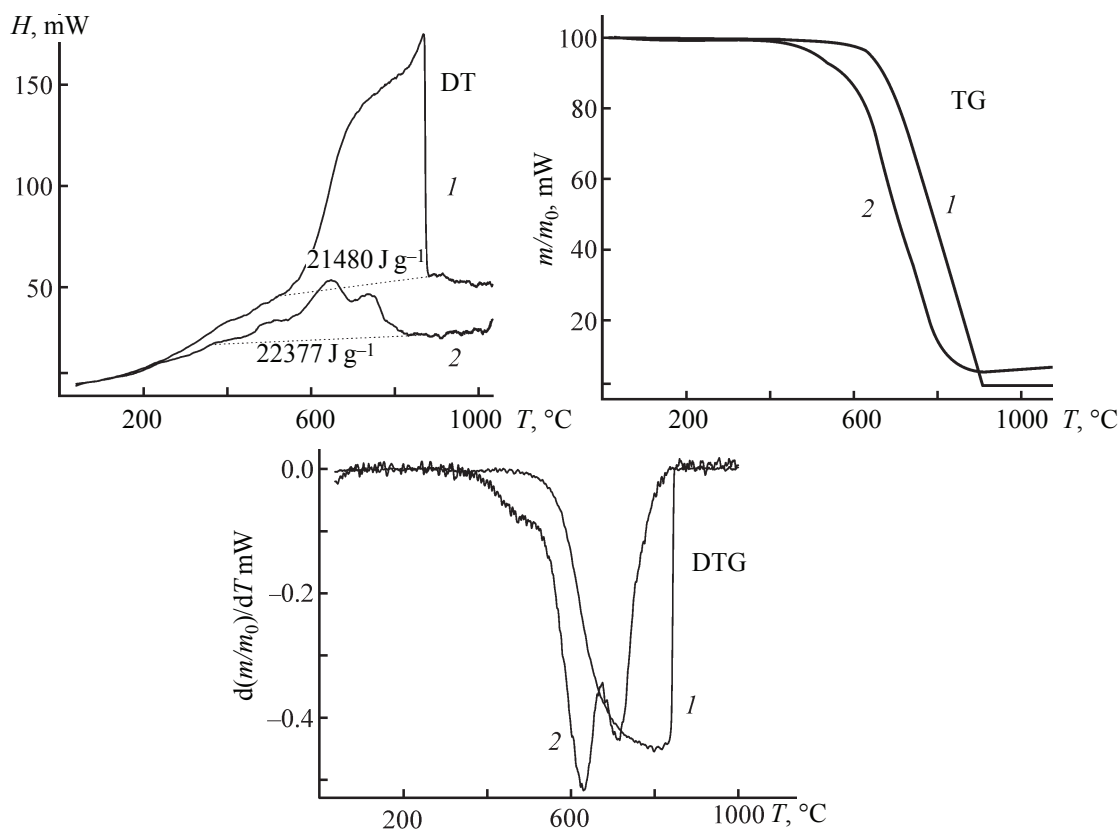


Fig. 1. Derivatograms obtained in air at a temperature raised at a constant rate of 10 deg min⁻¹. (*H*) Heat effect, (*m*, *m*₀) running and initial sample masses, and (*T*) Temperature. (*1*) Vulcan XC-72 carbon black and (*2*) TEG.

thermogravimetric (DTG) and differential thermal (DT) curves in the temperature ranges 450–500, 550–670, and 670–800°C. The loss of mass in these steps was about 11, 54, and 34%, respectively. This behavior is commonly attributed to the presence of three dispersed phases in the

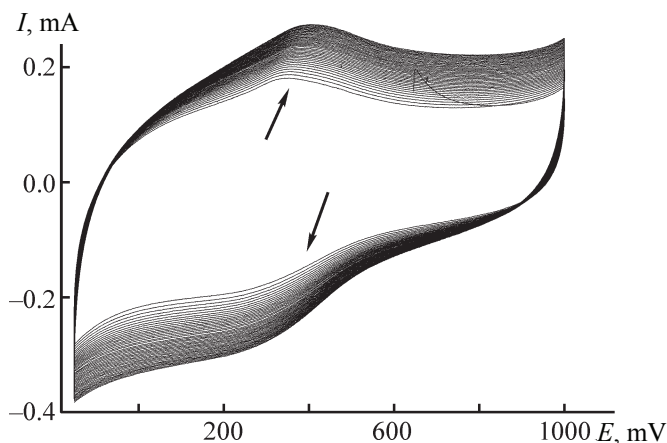


Fig. 2. Cyclic voltammograms of a TEG sample on a stationary disk electrode. Polarization rate 50 mV s⁻¹. (*I*) Current and (*E*) potential relative to a silver chloride reference electrode.

material. All the three effects in the differential thermal curve are exothermic. The material is mostly composed of two dispersed phases with combustion temperatures found from the peaks in the DTG curve to be 630 and 710°C. The combustion of Vulcan is characterized by a single step in the range 550–850°C, with the combustion rate being at a maximum at a temperature of about 800°C. The difference in the combustion temperatures can be accounted for by the different dispersities of the materials under study. It is noteworthy that the combustion heats have close values for these materials: 22.4 and 21.5 kJ g⁻¹ for TEG and Vulcan, respectively, but it is lower than the reference value for graphite, ~31 kJ g⁻¹ [21]. This can be attributed to the presence of surface groups of atoms on the developed surface of TEG and carbon black.

Electrochemical behavior. The family of cyclic voltammograms of TEG (Fig. 2) shows 41 cycles. Some specific features of the electrochemical behavior of TEG are noteworthy. First, there is quinone–hydroquinone equilibrium associated with the formation of quinone groups of atoms on the surface of the carbon material, which is manifested in the existence of the anodic and

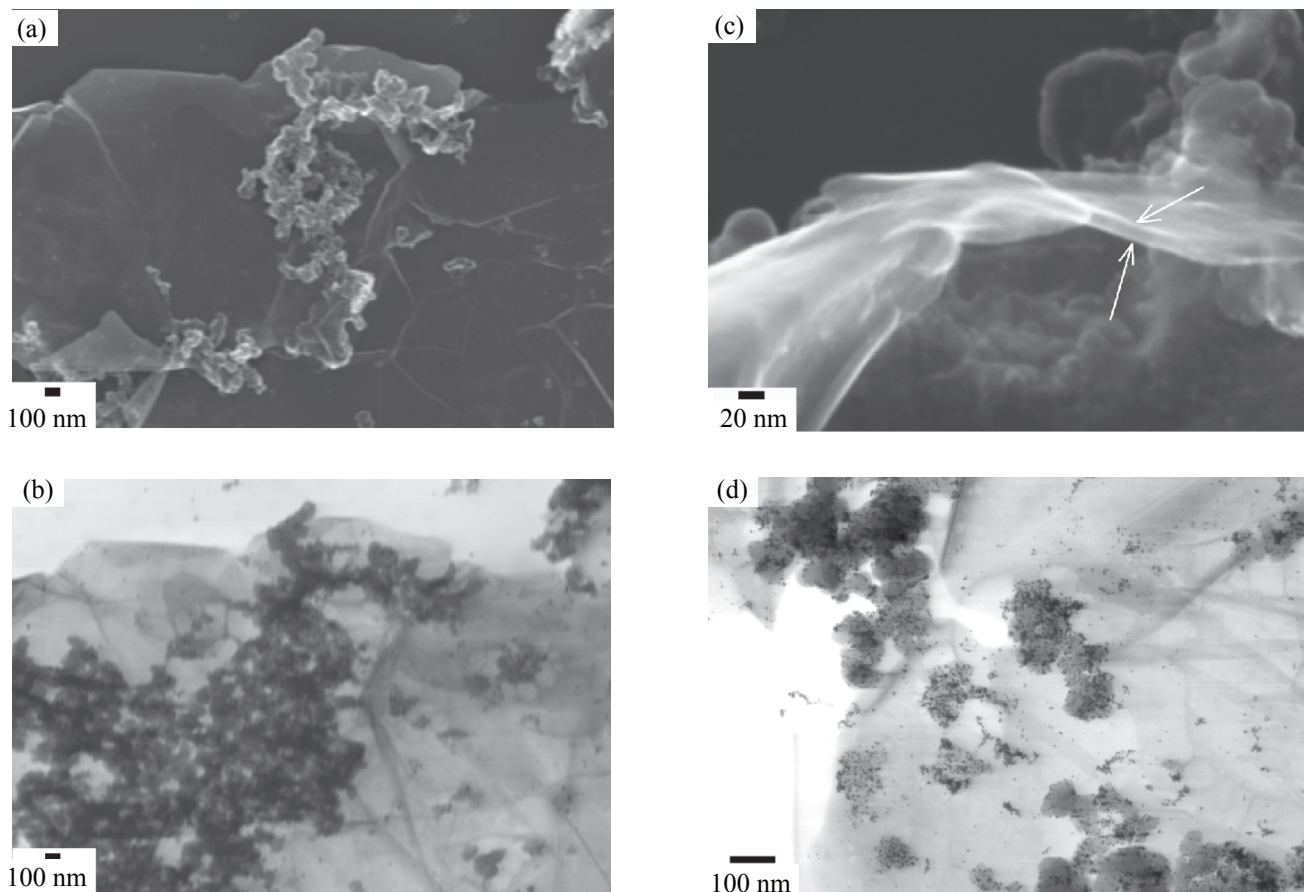


Fig. 3. (a, c) SEM and (b, d) TEM micrographs of the electrode material of composition (%): 30 Pt/C, 30 TEG, Nafion 40 (Figs. 1a and 1b show the same region).

cathodic current peaks (shown by arrows) [22, 23]. Second, the cyclic voltammograms become wider as the electrochemical action progresses (cycle number increases), which indicates that the surface area of the material grows. In addition, the cathodic peak is shifted to higher potential, and the anodic peak, to lower potentials. This demonstrates that the electrochemical quinone-hydroquinone process becomes less reversible: the rate constant of the process decreases. The table summarizes the dynamics of the characteristics of a sample in the course of the electrochemical treatment. It can be seen that the variation of the characteristics tends to saturate. This behavior of the material under an electrochemical treatment can be attributed to the further expansion of TEG, which is accompanied by an increase in the surface area and by an electrochemical functionalization that consists in partial oxidation with addition of oxygen-containing groups of atoms.

It is noteworthy that the presence of oxygen-containing groups of atoms in TEG, evidenced by CVA (Fig. 2), agrees with its combustion heat (which is lower than that of graphite).

Microscopic studies. Figure 3 shows micrographs of the material of the following composition (%): Pt/C 30, TEG 30, Nafion 40 (sample NANG-71).

Variation of characteristics of a TEG sample in the course of electrochemical treatment in 0.5 M H₂SO₄

Cycle no.	CVA width at 650 mV, mA	Cathodic peak potential	Anodic peak potential
		mV	
2	200	355	276
293	606	459	267
1073	628	465	262

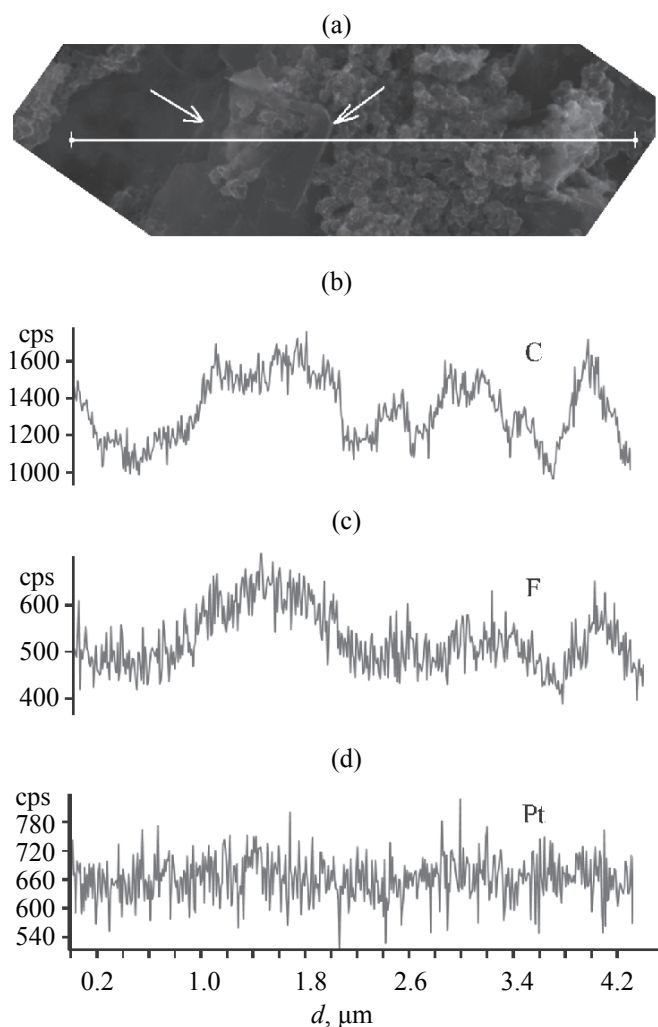


Fig. 4. (a) Micrograph with the scanning line and EDX maps of (b) carbon, (c) fluorine, and (d) platinum. (cps) Number of pulses in a second and (d) distance.

A graphite plane and platinized carbon black on this plane can be seen in Figs. 3a and 3b in the SEM and TEM images of the same part of the sample. The TEM image shows platinized carbon black on the back side of the graphite plate. Figure 3c shows the edge of the graphite plate (indicated by the arrow), wherefrom its thickness can be estimated to be ~ 15 nm. Because the interplanar

Scheme 1. Structural formula of Nafion.

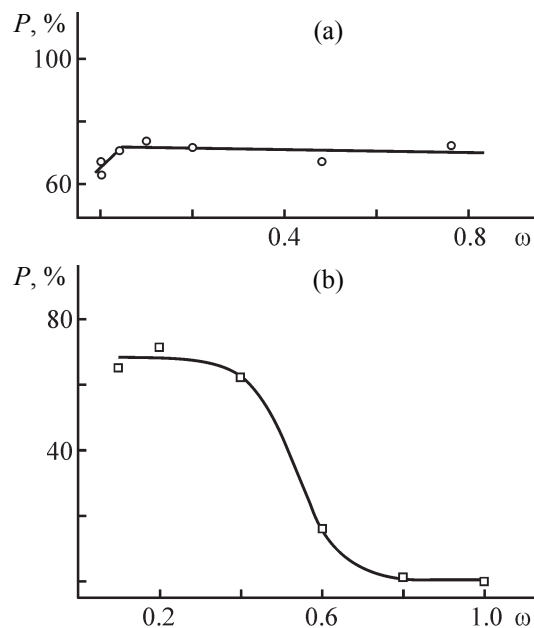
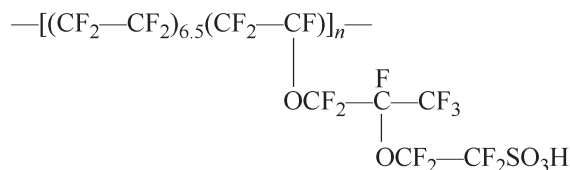


Fig. 5. Dependence of the porosity P of electrodes in (a) Vulcan-TEG-Nafion system at a 20% mass fraction of Nafion and (b) Pt/Vulcan-TEG-Nafion at a Pt/C : TEG mass ratio of 1 : 1 on the mass fraction ω of TEG.

space of graphite is 0.34 nm, this plate is constituted by 44 planes. Taking into account that the starting TEG has the form of substantially larger agglomerated particles, we can conclude that TEG is dispersed when the electrode material is prepared. Figure 3d shows platinum nanoparticles, dark dots situated both on the spherical agglomerates of carbon black and on the graphite plane. This fact indicates that platinum particles are redistributed, with the support changed, in the production of the electrode material.

The elemental composition of the material was studied in different parts of its surface by the EDX method (Fig. 4). The results obtained confirm the presence of elements introduced into the material. It is of interest to note in addition that the distributions of carbon and fluorine (which are indicative of the presence of Nafion because of being contained in its composition, see the structural formula) along the scanning line are similar and exhibit an undulate profile with a period of 0.4–1.6 μm . At the same time, platinum is distributed nearly uniformly (the signal intensity along the scanning line is nearly constant).

The structural formula of Nafion contained in a Nafion 117 membrane [24] is presented in Scheme 1.

Because carbon is contained in the material in the form of the carbon black (~18%), TEG (~30%), and Nafion (~5%) and platinum is mostly bound to carbon black, the change in the carbon concentration profile should be attributed to TEG. Because the profile of fluorine nearly reproduces that of carbon, this indicates that Nafion is mostly structurally bound to TEG. At the same time, the profile of fluorine is somewhat smoothed as compared with that of carbon, which indicates that there is a certain amount of Nafion in the form of structural elements unbound to TEG. Platinum is uniformly distributed within the material with its profile (Fig. 4d) only weakly reflecting that of carbon. The nature of the carbon profile can be attributed to the presence or absence of graphite plates in the scanning region and, accordingly, to the presence of pores with characteristic size equal to the period of the profile waves. For example, Fig. 4a shows a graphite plate (Indicated by arrows) corresponding to the range 1.1–1.9 μm in the case of distances and to the range of large values in the carbon profile (Fig. 4b).

Porosity. Figure 5a shows the dependence of the porosity of electrodes fabricated from the electrode material with varied content of TEG.

It can be seen in Fig. 5a that the porosity equal to ~70% is nearly independent of the content of TEG. At the same time, the porosity of a material containing no TEG is about 61%. This can be understood on the basis of microscopic data (see above). The micrographs show no so-called packets of TEG, with plates observed as split elements of graphite. As a result of the dispersion of TEG in the course of an ultrasonic processing of the material, its structural elements are transformed into thin plates (lamination), with carbon black and Nafion distributed on their surface. As a result, the porosity of the material varies only slightly in the range under study of the TEG concentrations. The structural role of Nafion in the material consists in the filling of voids between the carbon components, with the result that raising the mass fraction of Nafion leads to a significant decrease in porosity (Fig. 5b), with the porosity sharply decreasing as the fraction of Nafion increases from 0.4 to 0.6.

CONCLUSIONS

(1) A laboratory technique for obtaining electrodes containing platinized carbon black, thermally expanded graphite, and Nafion was developed. Fundamental aspects of the structuring in the system under consideration were examined and fundamental relationships between the

composition and structure of the composite electrode were determined.

(2) The electrochemical treatment of thermally expanded graphite results in that cyclic voltammograms become wider, which indicates that the surface area of the material becomes larger as a result of further expansion of thermally expanded graphite. This is accompanied by the electrochemical functionalization, which consists in a partial oxidation with addition of oxygen-containing groups of atoms.

(3) When a dispersion of catalytic ink is subjected to an ultrasonic treatment in preparing the electrode material, thermally expanded graphite is dispersed, with graphite layers split, and platinum nanoparticles are partly redistributed with a change of the support from carbon black to graphite planes.

(4) The distribution profiles of carbon and fluorine over the surface of the electrode material, found by the EDX method, have about the same undulate nature with a period of 0.4–1.6 μm . At the same time, platinum is distributed nearly uniformly (the signal intensity along the scanning direction is nearly the same). This indicates that Nafion is for the most part structurally bound to thermally expanded graphite.

(5) The nature of the carbon EDX profile is associated with the presence or absence of graphite plates in the scanning region and, accordingly, with the presence of pores having a characteristic size equal to the period of waves in the profile.

(6) The porosity of the electrode material at a constant Nafion concentration is about 68% and is nearly independent of the content of thermally expanded graphite. This is due to the lamination of thermally expanded graphite in the course of the ultrasonic treatment, with its structural elements transformed into thin plates (lamination) and carbon black and Nafion distributed over the surface of these plates.

(7) The porosity of the electrode material at a constant concentration of carbon components depends on the content of Nafion: raising the mass fraction of Nafion leads to a substantial decrease in porosity. The structural role of Nafion in the material consists in the filling of voids between the carbon components.

(8) New knowledge was obtained about the structuring processes occurring in composite electrodes for fuel cells upon introduction of thermally expanded graphite into their composition, which are necessary for fabrication

of electrodes with prescribed characteristics. This knowledge is of practical importance for development of scientific foundations for fabrication of electrodes for fuel cells with increased efficiency.

ACKNOWLEDGMENTS

The authors are grateful to the Department of structural studies at the Institute of Organic Chemistry, Russian Academy of Sciences, for electron-microscopic analyses of our samples. The experimental study was in part financially supported by the Russian Foundation for Basic Research (project no. 16-08-00797) and UMNIK program (project no. 10854gu/2016).

REFERENCES

1. Yilser Devrim and Ayhan Albostan, *J. Electron. Mater.*, 2016, vol. 45, no. 8, pp. 3900–3907.
2. Nedjeljko Seselj, Christian Engelbrekt, and Jingdong Zhang, *Sci. Bull.*, 2015, vol. 60(9), pp. 864–876.
3. Soo, L.T., Loh, K.S., Mohamad, A.B., et al., *Appl. Catal., A*, 2015, vol. 497, pp. 198–210.
4. Iwan, A., Malinowski, M., and Pasciak, G., *Renewable Sustainable Energy Rev.*, 2015, vol. 49, pp. 954–967.
5. Wang, X.-X., Zhou, Y.-Q., Zhu, Y., et al., *J. Chem. Chem. Eng. Croatia*, 2016, vol. 65 (5–6), pp. 259–264.
6. Alekseeva, O.K. and Fateev, V.N., *Altern. Energ. Ekol.*, 2015, vol. 7, pp. 14–36.
7. Miculescu, M., Miculescu, F., Thakur, V.K., and Voicu, S.I., *Polym. Adv. Technol.*, 2016, vol. 27, pp. 844–859.
8. Lee, J.Y., Lee, J.J., Rhim, H.R., et al., *Adv. Mater. Res.*, 2010, vols. 123–125, pp. 1107–1110.
9. Yakovlev, A.V., Finaenov, A.I., Zabud'kov, S.L., and Yakovleva, E.V., *Russ. J. Appl. Chem.*, 2006, vol. 79, no. 11, pp. 1741–1751.
10. Finaenov, A.I., Shpak, I.E., Afonina, A.V., et al., *Khim. Khim. Tekhnol.*, 2012, no. 4 (68), pp. 107–112.
11. Krasnova, A.O., Glebova, N.V., and Nechitailov, A.A., *Russ. J. Appl. Chem.*, 2016, vol. 89, no. 5, pp. 916–920.
12. Kovaleva, O.V., Kovalev, V.V., Duka, G.G., and Ivanov, M.V., *Probl. Region. Energet.*, 2011, no. 1, pp. 1–17.
13. <http://www.fuelcellstore.com/vulcan-xc72>.
14. RF Patent 2 581 382 (publ. 2016).
15. Zhang, J., *PEM Fuel Cell Electrocatalysts and Catalyst Layer*, Vancouver: Springer, 2008.
16. Nechitailov, A.A., Glebova, N.V., Koshkina, D.V., et al., *Tech. Phys. Lett.*, 2013, vol. 39, no. 9, pp. 762–766.
17. M. Barclay Satterfield, Paul W. Majsztrik, Hitoshi Ota, et al., *J. Polym. Sci., B*, 2006, vol. 44, pp. 2327–2345.
18. Kakaç, S., Pramuanjaroenkij, A., and Vasiliev, L., *Mini-Micro Fuel Cells: Fundamentals and Applications*. New York: Springer Science & Business Media, 2008.
19. Kachala, V.V., Khemchyan, L.L., Kashin, A.S., et al., *Uspekhi Khim.*, 2013, vol. 82, pp. 648–685.
20. Kashin, A.S. and Ananikov, V.P., *Russ. Chem. Bull. Int. Ed.*, 2011, vol. 60, pp. 2602–2607.
21. *Fizicheskaya entsiklopediya: Teplota sgoraniya* (Physical Encyclopedia: Combustion Heat), Prokhorov, A.M., Ed., Moscow: Sov. entsiklopediya, 1999.
22. Sadv, S.V., Sotskaya, N.V., and Kravchenko, T.A., *Zh. Fiz. Khim.*, 1993, vol. 67, pp. 2027–2029.
23. Glebova, N.V., Nechitailov, A.A., and Gurin, V.N., *Tech. Phys. Lett.*, 2011, vol. 37, no. 7, pp. 661–663.
24. Mingbao Feng, Ruijuan Qu, Zhongbo Wei, et al., *Sci. Rep.*, 2015, vol. 5 (9859), pp. 1–8.